ELSEVIER

Contents lists available at ScienceDirect

Chemical Engineering Journal

journal homepage: www.elsevier.com/locate/cej



Electrochemical and photoelectrochemical approaches for the selective removal, recovery, and valorization of chloride ions



Do-Hwan Nam, Dongho Lee, Kyoung-Shin Choi*

Department of Chemistry, University of Wisconsin-Madison, Madison, WI 53706, United States

HIGHLIGHTS

- Environmental concerns about increased chloride levels in freshwater resources.
- Electrochemical methods to selectively remove chloride.
- · Chloride removal coupled with electricity generation.
- Chloride removal coupled with hydrogen production.
- Electrochemical and photoelectrochemical methods to recover and valorize chloride.

ARTICLE INFO

Keywords: Chloride removal Chloride storage Chloride oxidation Water treatment Electrochemical cell Photoelectrochemical cell

ABSTRACT

Anthropogenic activities such as the use of water softeners and road deicers have artificially increased the Cl⁻ concentration in freshwater resources, threatening sustainable water ecosystems worldwide. Currently, there is no energy-efficient and sustainable method to selectively remove Cl⁻ from water to regulate the Cl⁻ concentration in water treatment processes. In this study, we report new electrochemical and photoelectrochemical strategies that can not only selectively remove Cl⁻ but also recover and valorize Cl⁻ to Cl₂, HOCl, and ClO⁻. These methods are based on the use of Bi as a Cl-storage/release electrode for the construction of Cl-removal and Cl-recovery cells. We demonstrate the operation of proof-of-concept electrochemical and photoelectrochemical cells where the Cl⁻ storage/release reactions are coupled with various reactions to generate electricity, fuels, and chemicals.

1. Introduction

In the past few decades, increased salinity of freshwater resources has become a serious global issue. Anthropogenic activities such as the use of water softeners and road deicers [1–5], disposal of wastewater treatment plant effluents [5,6], and agricultural practices have artificially elevated ionic concentrations in water well above their natural levels, threatening sustainable water ecosystems and resources worldwide [7–10]. The increase in the concentration of Cl⁻ in freshwater resources is particularly problematic as a high level of Cl⁻ is known to be harmful to aquatic life [11–13]. In addition, elevated Cl⁻ levels in freshwater resources and wastewater promote severe corrosion of pipelines and contribute to leaching of heavy metals such as Pb, Fe, and Cu from aging water infrastructure [14–16], which can adversely affect plants, animals and humans [17].

Currently, wastewater treatment plants are not equipped to regulate Cl^- levels, meaning that Cl^- is discharged into freshwater streams

[13], even when its concentration exceeds the limit recommended by the U.S. Environmental Protection Agency (EPA) (i.e. 860 mg/L for one-hour average and 230 mg/L for 96-hour average) [12]. All technologies that are currently available for Cl⁻ removal (e.g. reverse osmosis, electrodialysis) are cost-prohibitive for use in wastewater treatment applications because they cannot selectively remove Cl⁻; in order to decrease the Cl⁻ concentration, these technologies will also have to remove all other ions, which is unnecessary, and results in excessive energy consumption. Therefore, developing a cost-effective and energy-efficient method to enable the selective removal of Cl⁻ is imperative to alleviate the harmful environmental impacts of Cl⁻.

In the present study, we report new electrochemical strategies to selectively remove, recover, and valorize Cl⁻. Our strategies involve the construction of a Cl-removal cell and a Cl-recovery cell by exploiting the ability of Bi to electrochemically store and release Cl⁻ through the following reversible reaction (Eq. (1)) [18]:

E-mail address: kschoi@chem.wisc.edu (K.-S. Choi).

^{*} Corresponding author.

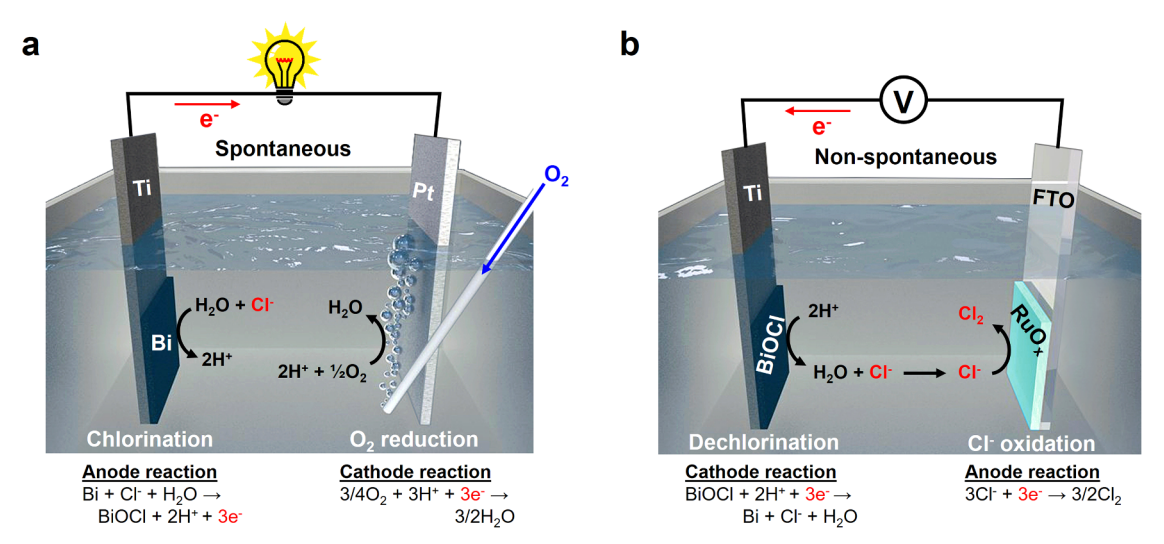


Fig. 1. Schemes showing the operation of (a) a Cl-removal cell where the oxidation of Bi to BiOCl is coupled with O_2 reduction and (b) a Cl-recovery cell where the reduction of BiOCl to Bi is coupled with Cl^- oxidation. The Cl-removal cell generates electricity while the Cl-recovery cell consumes electricity.

Bi(s) + Cl⁻(aq) + H₂O(l)
$$\rightleftharpoons$$
 BiOCl(s) + 2H⁺(aq)
+ 3e⁻(E° = 0.160 V vs SHE) (1)

In the Cl-removal cell (Fig. 1a), Cl⁻ storage by Bi (oxidation of Bi to BiOCl) is paired with O_2 reduction to water $(O_2(g) + 4H^+(aq) + 4e^-)$ \Rightarrow 2H₂O(*l*), E° = 1.23 V vs SHE). O₂ reduction is an easily accessible reaction as water resources under ambient conditions typically contain dissolved O_2 . If necessary, the amount of O_2 in the solution can be easily increased by purging with air or O2 gas. As the reduction potential of O₂ (cathode reaction) is more positive than the oxidation potential of Bi to BiOCl (anode reaction), the cell voltage ($E_{cell} = E_{cathode} - E_{anode}$) is positive, meaning that ΔG for the overall reaction is negative (ΔG 0). Thus, the Cl-removal cell operates spontaneously; while Cl⁻ is removed from the feedwater, the cell also generates an electrical energy output, which is unprecedented in the field of Cl⁻ removal. Once Bi is fully converted to BiOCl, Cl - can be released from BiOCl in a Cl-recovery cell (Fig. 1b) to regenerate Bi. In the Cl-recovery cell, the release of Cl from BiOCl (reduction of BiOCl to Bi) is paired with Cl oxidation. The overall reaction occurring in the Cl-recovery cell is nonspontaneous ($\Delta G > 0$), and, therefore, the operation of the Cl-recovery cell will require an energy input. However, the Cl-recovery cell also generates industrially valuable Cl2 gas or HOCl/ClO that is commonly used as a disinfectant. Thus, our new electrochemical approach provides an integrated strategy to selectively remove, recover, and valorize Cl that can be used for various municipal and industrial water treatment processes. Here, we demonstrate the construction and operation of proof-of-concept Cl-removal and Cl-recovery cells. We also show the possibility of using a semiconductor anode (photoanode) to construct a photoelectrochemical Cl-recovery cell that utilizes solar energy to reduce the electrical energy input required for the operation of the cell. Our approach will stimulate further development of electrochemical and photoelectrochemical processes for efficient and practical Cl removal and utilization.

2. Materials and methods

2.1. Materials

NaCl (99%, Sigma-Aldrich), BiCl₃ (\geq 98%, Sigma-Aldrich), Polyethylene glycol (PEG) (Molecular weight of 6000, USB Corporation), HCl (37%, Sigma-Aldrich), RuCl₃·xH₂O (35–40%, Acros), NH₄Cl (\geq 99.5%, Sigma-Aldrich), Bi(NO₃)₃·5H₂O (98%, Sigma-Aldrich), KI (99%, Sigma-Aldrich), lactic acid (85–90%, Alfa Aesar), HNO₃ (98%, Sigma-Aldrich), p-benzoquinone (98%, Sigma-Aldrich), dimethyl

sulfoxide (99.9%, BDH), VO(acac) $_2$ (98%, Sigma-Aldrich), NaOH (97%, Sigma-Aldrich), (NH $_4$) $_2$ [TiO(C $_2$ O $_4$) $_2$]·H $_2$ O (99.998%, Sigma-Aldrich), NH $_4$ OH (28.0–30.0%, Sigma-Aldrich), graphite (< 20 μ m, Sigma-Aldrich), KNO $_3$ (99.0%, Alfa Aesar), and ethanol (Pharmco, 200 proof) were used without further purification. Deionized (DI) water (Barnstead E-pure water purification system, resistivity > 18 M Ω cm) was used to prepare all solutions.

2.2. Preparation of Bi foam electrodes

Bi electrodes used in this study were prepared by electrodeposition following the procedure reported in a previous study [18]. An undivided three-electrode cell consisting of a Ti sheet working electrode, a Pt foil counter electrode, and an Ag/AgCl reference electrode (4 M KCl) was used. The Ti sheet was masked to expose an area of 1 cm². An aqueous solution containing 14 mM BiCl₃, 1.4 M HCl, and 2.5 g/L PEG 6000 was used as the plating solution. A potentiostatic deposition was performed by applying a constant potential of -2.6 V vs Ag/AgCl for 1 min 50 s to deposit Bi (Bi³⁺ + 3e⁻ \rightarrow Bi, E^o = 0.286 V vs SHE). During the deposition the solution was stirred at 300 rpm. After deposition, the Bi electrodes were rinsed with water and dried in air. The average mass of Bi in the electrodes was approximately 1.25 mg/cm², which was determined by weighing the Ti substrate before and after the electrodeposition of Bi. A VMP2 multichannel potentiostat (Princeton Applied Research) was used for all electrodeposition and electrochemical studies.

2.3. Preparation of RuO_x electrodes

Electrodeposition of ${\rm RuO_x}$ electrodes was performed in a solution containing a mixture of 30 mL DI water and 10 mL ethanol with 5 mM ${\rm RuCl_3} \times {\rm H_2O}$, 25 mM p-benzoquinone, and 0.1 M ${\rm NH_4Cl}$. The pH of the as-prepared solution was 2.44 and was not adjusted further. An undivided three-electrode cell was used for the deposition and consisted of a fluorine-doped tin oxide (FTO) (Hartford Glass) working electrode, a Pt counter electrode, and an Ag/AgCl (4 M KCl) reference electrode. The Pt counter electrode was prepared by sputter coating 100 nm of Pt on top of a 20 nm Ti adhesion layer on a clean glass slide (LGA Thin Films). The lateral dimensions of the FTO electrode used in this study were 1 cm \times 1.2 cm. A galvanostatic deposition was performed at -2 mA/cm² to pass a total charge of 60 mC/cm². Under electrical bias, the reduction of p-benzoquinone elevates the local pH in the vicinity of the working electrode, resulting in the precipitation of ${\rm RuO_x}$ on the surface of the working electrode. As-deposited electrodes were rinsed with

ethanol and dried in air. The resulting electrodes were annealed by hybrid microwave annealing (HMA) [35] for 2 min in a microwave oven (AmazonBasics, 700 W) to enhance the stability of RuO_x . A Pyrex beaker filled with graphite powder was used as the susceptor during the microwave treatment.

2.4. Preparation of BiVO₄ electrodes

First, BiOI electrodes were electrodeposited to serve as precursor films to form nanoporous BiVO₄ electrodes. The deposition mechanism and conditions for the deposition of BiOI have been reported previously [28,29]. The plating solution used for the deposition was a 50 mL aqueous solution containing 15 mM Bi(NO₃)₃·5H₂O, 400 mM KI, and 30 mM lactic acid. Prior to the deposition, 20 mL of ethanol containing 46 mM p-benzoquinone was slowly added. The mixed aqueous/ethanol solution was stirred for several min until its pH stabilized. The final pH was adjusted to 3.70 ± 0.1 by adding fresh HNO₃. A typical threeelectrode cell was used for electrodeposition. An FTO working electrode, a Pt counter electrode, and an Ag/AgCl (4 M KCl) reference electrode were used. The potentiostatic deposition was performed in two steps. First, a potential of -0.35~V vs Ag/AgCl was applied for 20~sas the nucleation step and then, a constant potential of -0.10 V vs Ag/ AgCl was applied to pass 0.35 C/cm². As-deposited electrodes were rinsed with water and dried in air. The BiOI electrodes were converted to BiVO₄ by annealing in air at 450 °C for 2 h (ramp rate = 2 °C/min) after covering the film surface (lateral dimensions of the film = 1.0 cm \times 1.2 cm) with 65 μ L/cm² of a dimethyl sulfoxide solution containing 200 mM VO(acac)₂. After the conversion, excess V₂O₅ present in the BiVO₄ electrode was removed by soaking the film in a 1 M NaOH solution for 30 min while stirring at 400 rpm. The electrode was rinsed with water and dried with an air stream.

2.5. Electrodeposition of TiO2 on BiVO4 electrodes

TiO₂ was electrochemically deposited on the BiVO₄ electrodes based on the method reported in the recent study [29]. A plating solution was prepared by adding 10 mL of ethanol containing 0.16 M p-benzoquinone to 30 mL of an aqueous solution containing 0.107 M (NH₄)₂[TiO (C₂O₄)₂]·H₂O. Then, the pH was adjusted to 4.5 by adding a few drops of NH₄OH solution with vigorous stirring to minimize the precipitation of Ti hydroxides that can occur upon a sudden pH increase. An undivided three-electrode cell with a BiVO4 working electrode, a Pt counter electrode, and an Ag/AgCl (4 M KCl) reference electrode was used for the electrodeposition of TiO_2 . A constant current of -3 mA/ cm² was applied to pass 50 mC/cm², and then the as-prepared BiVO₄/ TiO₂ electrodes were rinsed with ethanol and dried with a gentle stream of air. The resulting electrodes were HMA treated for 2 min in a microwave oven using a Pyrex beaker filled with graphite powder as the susceptor. The resulting TiO2 layer was amorphous. The thickness of the TiO2 layer (~10 nm thick) and the ability of the conformally coated TiO₂ layer to chemically protect BiVO₄ were reported in a previous study [29].

2.6. Characterization

The morphology of the electrodes was examined using a LEO Supra55 VP Scanning Electron Microscope (SEM) at an accelerating voltage of 2 kV. The crystallinity and purity of the electrodes were examined by X-ray diffraction (XRD) using a Bruker D8 Advanced X-ray diffractometer (Ni-filtered Cu K_{α} -radiation, $\lambda=1.5418$ Å). The presence of the TiO $_2$ layer on the BiVO $_4$ electrode was investigated by X-ray photoelectron spectroscopy (XPS) using a K-Alpha X-ray photoelectron spectrometer (Thermo Scientific) with a monochromatized Al $K\alpha$ X-ray source (1486.68 eV).

2.7. Electrochemical testing

The Cl-removal cell was a custom built two-compartment Teflon cell. The anode compartment and cathode compartment were divided by a cation exchange membrane (Nafion 117, FuelCellStore). The area of the cation exchange membrane exposed to the electrolyte was 5.7 cm². Both compartments contained 10 mL of 0.6 M NaCl as the electrolyte. The electrolytes were not circulated or stirred during cell operation. When necessary, the solution in the cathode compartment was purged with high-purity O2 gas during cell operation. A Bi foam electrode (geometric area of 1 cm²) was used as the anode and Pt foil (geometric area of 7.5 cm²) was used as the cathode. The distance between the Bi and Pt electrodes was 1.5 cm. The Cl-removal cell was operated galvanostatically at 1 mA/cm² (based on the geometric area of Bi). An Ag/AgCl (4 M KCl) reference electrode was immersed in the anode compartment near the Bi electrode to monitor changes in the individual potentials of the Bi and Pt electrodes during cell operation. To verify that the Cl-removal cell generated electrical energy during operation, an additional experiment was performed where a lightemitting diode (LED) bulb was connected to the Bi and Pt electrodes. In this experiment, since the voltage generated by the single cell is not high enough to illuminate an LED bulb, the bulb was connected through a pulse frequency modulation control DC/DC boost controller chip (SenMod) that steps up the voltage (while stepping down the current) output to 5 V. The Cl-recovery cell was an undivided cell composed of a BiOCl electrode (geometric area of 1 $\mbox{cm}^2)$ as the cathode and an \mbox{RuO}_x electrode (geometric area of 1 cm2) as the anode. Two-types of electrolytes, 0.6 M NaCl and 70 mM HCl, were used to examine the effects of pH on the BiOCl reduction kinetics. The cell was operated galvanostatically at 1 mA/cm². The individual potentials of the cathode and the anode were monitored against an Ag/AgCl (4 M KCl) reference electrode during cell operation.

2.8. Determination of Cl⁻ removal efficiency

The actual concentrations of Cl⁻ in the solution were measured by a chloride ion meter (Horiba 6560-10C). An undivided three-electrode cell consisting of a Bi working electrode, a Pt foil counter electrode, and an Ag/AgCl reference electrode (4 M KCl) was used. Potentiostatic oxidation of Bi to BiOCl was performed by applying a constant potential of 0.6 V vs Ag/AgCl and the Cl - concentration in the solution was analyzed after passing a charge of 0, 10, 20, 30, 40, and 50 C. Since the size and, therefore, the Cl removal capacity of the Bi electrode used in this study was limited, a 60 mM NaCl solution rather than a 0.6 M NaCl solution was used for this experiment. Lowering the initial Cl- concentration has the effect of increasing the percentage of Cl- removed for a given charge passed and results in more reliable measurements by the chloride ion meter. Before the measurement, 0.1 M KNO₃ was dissolved in the solutions as a supporting electrolyte to provide optimum solution conductivity for the operation of the Cl-selective electrode in the chloride ion meter.

2.9. Photoelectrochemical measurements

The photoelectrochemical Cl-recovery cell was constructed using a BiOCl cathode and a BiVO $_4$ /TiO $_2$ photoanode (geometric area of 1 cm 2) with all other components the same as those of the electrochemical Cl-recovery cell. The light was generated from an Oriel LCS-100 solar simulator (150 W Xe arc lamp) equipped with an air mass 1.5 global (AM 1.5G) filter, and passed through an infrared (water) filter (Newport) and neutral density filters. Illumination was through the FTO side of the BiVO $_4$ electrode (back-side illumination). The intensity of the light was calibrated to be one sun (100 mW/cm 2) at the surface of the FTO substrate (before the light passes through the FTO) using a NREL certified GaAs reference cell (PV Measurement). The illuminated area of BiVO $_4$ was 1 cm 2 . The cell was operated galvanostatically at 1 mA/cm 2 .

The individual potentials of the photoanode and the cathode were monitored against an Ag/AgCl (4 M KCl) reference electrode during cell operation. Additionally, J-V plots of a BiVO₄/TiO₂ photoanode were obtained in 0.6 M NaCl and 70 mM HCl using a three-electrode cell to demonstrate the general photoelectrochemical performance. A Pt counter electrode and an Ag/AgCl (4 M KCl) electrode were used in an undivided cell with the same aforementioned illumination conditions.

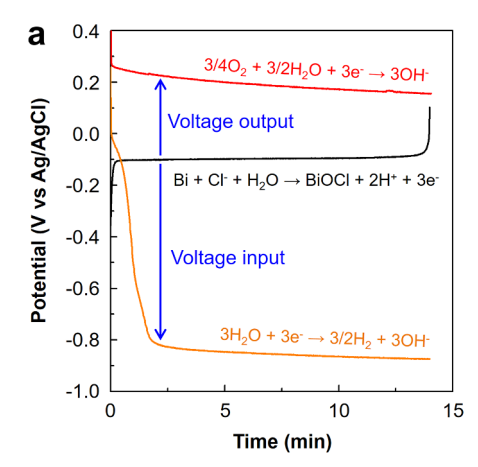
3. Results and discussion

3.1. Electrochemical Cl-removal cell

The Cl-removal cell is composed of a Bi anode performing the Cl⁻ storage reaction and a Pt cathode performing O_2 reduction. The Bi electrode was prepared as a nanocrystalline foam electrode using a previously reported electrodeposition method [18,19]. The SEM images and XRD pattern of the Bi electrode can be found in Fig. S1. The Pt electrode used in this study was commercially available Pt foil. As the goal of this study is not to achieve efficient and inexpensive O_2 reduction but rather to demonstrate the operation of a proof-of-concept Cl-removal cell, we chose Pt as the simplest possible cathode that can perform O_2 reduction. When the Cl-removal cell is developed further, the Pt electrode can be replaced with a more practical and efficient electrode that has been identified from the field of O_2 reduction [20,21].

The anode and the cathode compartments of the Cl-removal cell both contained 0.6 M NaCl and were divided by a cation exchange membrane. The catholyte was purged with O_2 before and during the cell operation. Fig. 2a shows the potential-time (V-t) plot of the Cl-removal cell when the cell was operated galvanostatically at 1 mA/cm². During operation, the potentials of the Bi anode and the Pt cathode were measured individually against an Ag/AgCl reference electrode that was located in the anode compartment near the Bi electrode. This allowed both the cell voltage ($E_{\rm cell} = E_{\rm Pt~cathode}$ - $E_{\rm Bi~anode}$) and the individual electrode potentials to be monitored over time.

During cell operation, the average potential applied to the Bi anode to oxidize Bi to BiOCl was -0.08 V vs Ag/AgCl [18,22]. The sharp increase in the potential observed at t=14 min (equivalent to passing a charge of 0.84 C) indicates that the conversion of Bi to BiOCl was complete. (When the conversion of Bi to BiOCl is complete, the potential becomes more positive to induce a new oxidation reaction to maintain the applied current of 1 mA/cm^2 .) Considering the theoretical



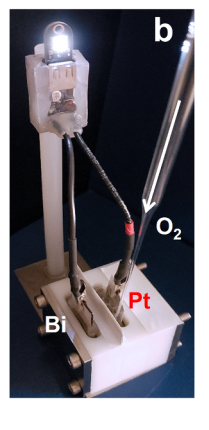


Fig. 2. (a) V-t plots for the Bi anode (black) and Pt cathode for O_2 reduction (red) and water reduction (orange) when the Cl-removal cell was operated at 1 mA/cm². (b) A photograph showing an LED bulb illuminated during the cell operation confirming that electrical energy was generated by the Cl-removal cell when O_2 reduction was used as the cathode reaction. (For interpretation of the references to colour in this figure legend, the reader is referred to the web version of this article.)

Cl $^-$ removal capacity of 1 g of Bi (169.6 mg/g_{Bi}) and the amount of Bi contained in the Bi electrode (1.25 mg), passing a charge of 0.84 C to complete the reaction (equivalent to storing 0.103 mg of Cl $^-$) indicates that 49% of the Bi electrode is electrochemically active. The formation of BiOCl was also confirmed by XRD (Fig. S2). Additionally, we monitored the change in Cl $^-$ concentration of the electrolyte as a function of charge passed to confirm $\sim 100\%$ Faradaic efficiency for Cl $^-$ removal by the Bi electrode (Fig. S3).

The average potential applied to the Pt cathode during O_2 reduction was 0.23 V vs Ag/AgCl. As expected, the cathode potential was more positive than the anode potential applied to the Bi electrode. This means that the overall reaction is spontaneous, and the Cl-removal cell can generate an electrical energy output. (The average output voltage of the cell reported here is 0.31 V at 1 mA/cm².) In order to visualize the electrical energy generation, we connected a small LED bulb to the Cl-removal cell and the bulb was indeed illuminated when the Cl-removal cell was operated without any external electrical energy input (Fig. 2b). This confirms that our Cl-recovery cell can generate electricity concurrently with Cl $^-$ removal.

Another possible cathode reaction that can be coupled with Cl storage by Bi is water reduction to H_2 (2H⁺(aq) + 2e⁻ \rightarrow H₂(g), E° = 0.00 V vs SHE). In this case, the water reduction potential is more negative than the oxidation potential of Bi and so the overall reaction is non-spontaneous and requires an energy input. However, this cell generates H₂ as a valuable product while simultaneously removing Cl⁻. Therefore, for some applications, a Cl-removal cell that couples Clremoval with H₂ production may be preferred. One possible advantage of producing H₂ in the Cl-removal cell rather than in a typical water splitting electrolyzer where H2 production is coupled with O2 production is that the former requires a smaller thermodynamic cell voltage (E $^{\circ}_{\rm cell}$ = -0.16 V for the Cl-removal cell and E $^{\circ}_{\rm cell}$ = -1.23 V for a water splitting electrolyzer). This means that the Cl-removal cell can produce H₂ with a lower voltage than that required for a typical electrolyzer. Additionally, H2 is the only gas produced in the Cl-removal cell (i.e. no O2 evolution) and may simplify the collection of H2.

The V-t plot of the Cl-removal cell operated galvanostatically at $1~\text{mA/cm}^2$ using water reduction as the cathode reaction is shown in Fig. 2a. The average potential applied to the Pt cathode performing water reduction was -0.85~V vs Ag/AgCl, resulting in an average cell voltage of -0.77~V.

3.2. Electrochemical Cl-recovery cell

The BiOCl obtained when Cl^- is stored by Bi in the Cl-removal cell can be converted back to Bi in the Cl-recovery cell through the release of Cl^- from BiOCl (reverse reaction of Eq. (1)). In this cell, the reduction of BiOCl is coupled with Cl^- oxidation $(2Cl^-(aq) \rightleftharpoons Cl_2(g) + 2e^-, E^\circ = 1.36 \text{ V vs SHE})$ by an RuO_x electrode. This enables direct valorization of Cl^- released from the cathode into valuable products (Fig. 1b). We used an RuO_x electrode to demonstrate the operation of a proof-of-concept cell because it is the simplest catalytic electrode for Cl^- oxidation [23,24]. When this cell is developed further, RuO_x can be replaced with an electrode that has been optimized for Cl^- oxidation [24]. The RuO_x electrode used in this study was prepared by electrodeposition as an amorphous, thin film-type electrode (Fig. S4). The current density-potential (J-V) plots of the RuO_x electrode for Cl^- oxidation can be found in Fig. S5.

The major product of Cl $^-$ oxidation varies depending on the pH of the solution. For example, at pH < \sim 3, Cl $_2$ gas is the major product. At pH > \sim 3, Cl $_2$ reacts with water to produce HOCl (Eq. (2)). When the solution pH is higher, HOCl can be further deprotonated to form ClO $^-$ (pK $_a$ = 7.53) (Eq. (3)) [25].

$$\operatorname{Cl}_2(g) + \operatorname{H}_2\operatorname{O}(l) \rightleftharpoons \operatorname{H}^+(aq) + \operatorname{HOCl}(aq) + \operatorname{Cl}^-(aq)$$
 (2)

$$HOCl(aq) + H2O(l) \rightleftharpoons ClO^{-}(aq) + H3O^{+}(aq)$$
(3)

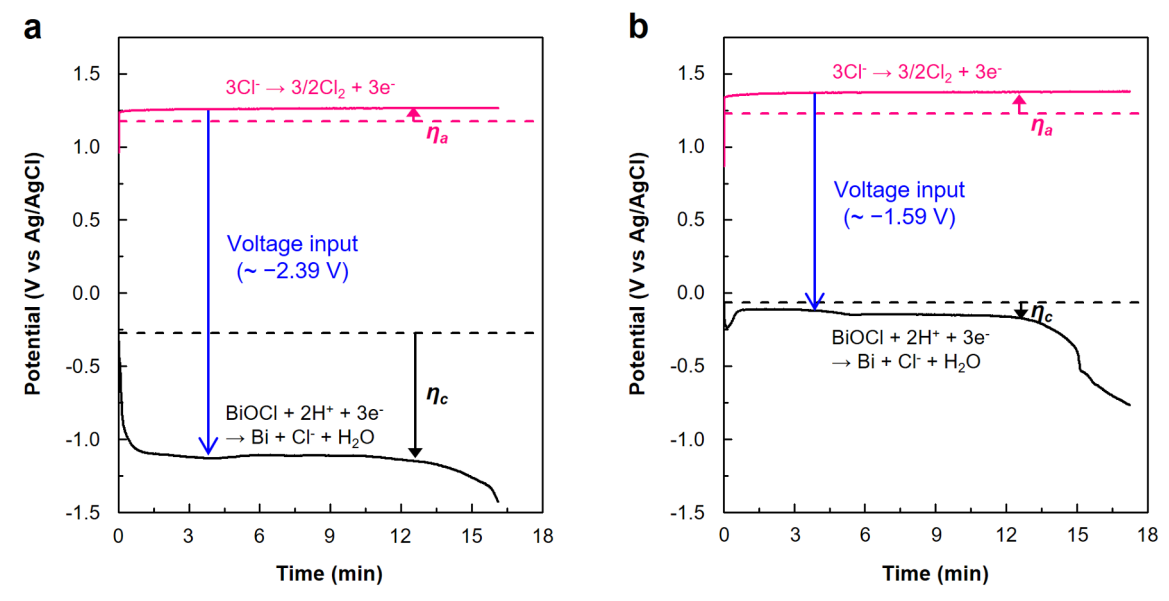


Fig. 3. V-t plots for the BiOCl cathode and the RuO_x anode when the Cl-recovery cell was operated at 1 mA/cm² in (a) 0.6 M NaCl and (b) 70 mM HCl. The equilibrium oxidation potential of Cl⁻ to Cl₂ and equilibrium reduction potential of BiOCl to Bi are displayed by the dashed pink lines and dashed black lines, respectively (η_a : anodic overpotential, η_c : cathodic overpotential). For simplicity, the equilibrium potentials for Cl⁻ oxidation were calculated assuming that the partial pressure of Cl₂ is 1 atm and ignoring the pH-dependent chemical reactions that Cl₂ undergoes in aqueous solutions. (For interpretation of the references to colour in this figure legend, the reader is referred to the web version of this article.)

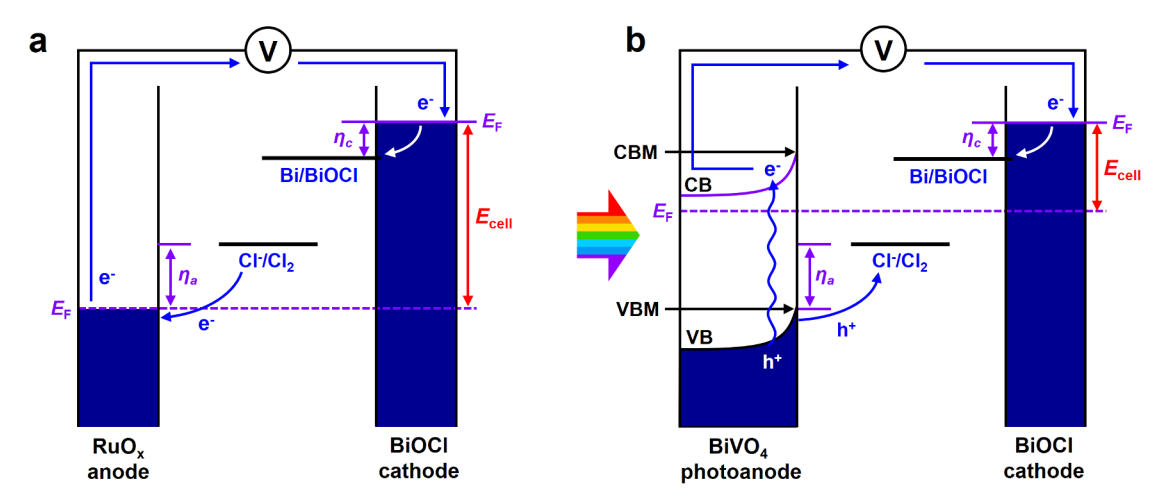


Fig. 4. Energetics of (a) the electrochemical cell composed of a RuO_x anode and BiOCl cathode and (b) the photoelectrochemical cell composed of a $BiVO_4$ photoanode and BiOCl cathode under illumination (CB: conduction band, VB: valence band, CBM: conduction band minimum, VBM: valence band maximum, E_F : Fermi level, η_a : anodic overpotential, η_c : cathodic overpotential, E_{cell} : cell voltage).

Water oxidation that is thermodynamically more favorable than Cl^- oxidation [26] can also occur at the anode as a competing reaction. However, the kinetics for Cl^- oxidation are reported to be faster and Cl^- oxidation can dominate on RuO_x [25,27].

Fig. 3a shows the V-t plot when the Cl-recovery cell was operated in 0.6 M NaCl at 1 mA/cm². The average potential applied to the BiOCl cathode was -1.12 V vs Ag/AgCl. The negative shift of the potential at t = 15 min indicates that the reduction of BiOCl to Bi was complete. The complete conversion of BiOCl to Bi was verified by XRD (Fig. S6a); the XRD pattern shows the disappearance of BiOCl peaks and restoration of Bi peaks.

The average potential applied at the RuO_x anode during Cl^- oxidation was 1.25 V vs Ag/AgCl, resulting in an average cell voltage of ~ -2.39 V. We note that the observed cell voltage is significantly higher than the equilibrium cell voltage calculated for the given solution composition and pH ($E^e_{anode}=1.37$ V vs SHE, $E^e_{cathode}=-0.076$ V vs SHE, and $E^e_{cell}=-1.446$ V). The equilibrium potentials for the

anode and the cathode reactions are indicated as dashed lines in Fig. 3a. The difference between the experimentally observed potential and the equilibrium potential is the overpotential that is required to achieve a current of 1 mA/cm². Fig. 3a clearly shows that the overpotential required for the oxidation of Cl^- to Cl_2 (η_a) was not significant and it is the high overpotential required for the reduction of BiOCl to Bi (η_c) that is responsible for the large experimentally measured cell voltage. Previously, it was reported that the kinetics for the reduction of BiOCl to Bi are very slow in neutral conditions but improve considerably in acidic conditions. This is because the reduction of BiOCl to Bi involves the release of O²⁻ as well as Cl⁻ from the BiOCl lattice and the kinetics for O²⁻ release may be faster when H⁺ rather than H₂O can serve as an O2- acceptor [18]. Indeed, when the same Cl-recovery cell was operated at 1 mA/cm² in 70 mM HCl, the potential applied to the BiOCl cathode shifted to the positive direction by 0.9 V and the average cell voltage was reduced to ~ -1.59 V (Fig. 3b). The equilibrium potential of the Bi/BiOCl reaction in the acidic solution is also indicated in

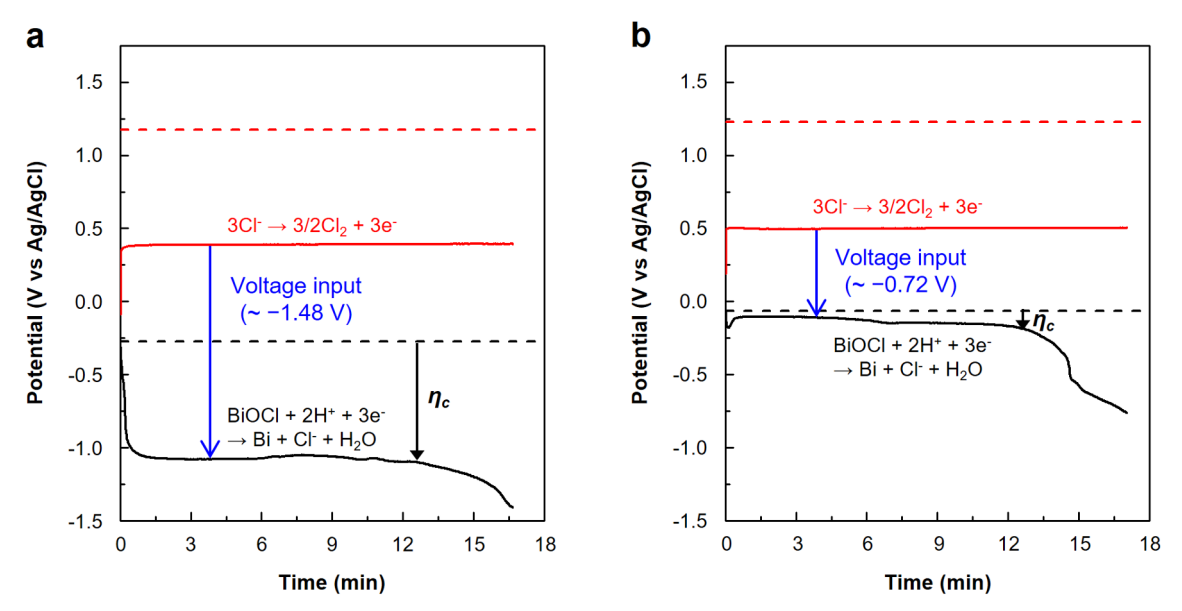


Fig. 5. V-t plots for the BiOCl cathode and the BiVO₄/TiO₂ photoanode when the photoelectrochemical Cl-recovery cell was operated at 1 mA/cm² in (a) 0.6 M NaCl and (b) 70 mM HCl. The equilibrium oxidation potential of Cl⁻ to Cl₂ and equilibrium reduction potential of BiOCl to Bi are displayed by the dashed red lines and dashed black lines, respectively. (For interpretation of the references to colour in this figure legend, the reader is referred to the web version of this article.)

Fig. 3b as a dashed black line so that the decrease in η_c can be easily recognized. The XRD pattern of the BiOCl electrode after the completion of the Cl⁻ release reaction in the acidic solution also confirmed the disappearance of BiOCl peaks and reappearance of Bi peaks (Fig. S6b).

3.3. Photoelectrochemical Cl-recovery cell.

An effective strategy that can be used to drastically decrease the energy required to operate the Cl-recovery cell is to replace the anode with a photoanode that can utilize solar energy to operate the cell (Fig. 4). Under illumination, electrons from the valence band (VB) of the photoanode are excited to the conduction band (CB). The holes that are generated in the VB can oxidize Cl - if the valence band maximum (VBM) is more positive than the potential required to oxidize Cl⁻. The electrons in the CB of the photoanode are transferred to the cathode and are used to reduce BiOCl to Bi. If the Fermi level of the photoanode under illumination is more negative than the potential required to reduce BiOCl, no additional energy input is required to operate the cell. However, if the Fermi level of the photoanode is more positive than the potential required to reduce BiOCl, an additional energy input will be necessary. The voltage required to operate the cell in this case is not the difference between the potential needed to reduce BiOCl and the potential needed to oxidize Cl - (Ecell in Fig. 4a) but the difference between the potential needed to reduce BiOCl and the Fermi level of the photoanode under illumination (E_{cell} in Fig. 4b). Therefore, the use of a photoanode results in a significant decrease in E_{cell}.

In this study, n-type nanoporous BiVO₄ was chosen as the photo-anode to construct a proof-of-concept photoelectrochemical Cl-recovery cell. The VBM of BiVO₄ is 2.4 V vs RHE, and, therefore, photogenerated holes in the VB of BiVO₄ have sufficient overpotential to perform Cl⁻ oxidation. The flatband potential (the maximum Fermi level that can be achieved under illumination) of BiVO₄ used in this study is ~0.2 V vs RHE [28–31]. This potential is slightly more positive than the potential required to reduce BiOCl to Bi. Thus, operation of the photoelectrochemical Cl-recovery cell will still require an additional energy input to enable the desired electrochemical reactions and provide necessary kinetic overpotentials. However, BiVO₄ was chosen for this study because it is one of the most efficient photoanodes that can utilize visible light while having a flatband potential near the reduction potential of BiOCl [30,31]. Additionally, BiVO₄ has been previously utilized for

photoelectrochemical ${\rm Cl}^-$ oxidation [32–34]. Therefore, ${\rm BiVO}_4$ is a good candidate for the construction of a proof-of-concept photoelectrochemical ${\rm Cl}$ -recovery cell.

The BiVO₄ electrode used in this study was prepared using a method reported previously [28]. SEM images and XRD patterns of the BiVO₄ photoanode used in this study can be found in Fig. S7 and 8. Before being used in the Cl-recovery cell, a thin (~10 nm) TiO2 coating layer was conformally electrodeposited on the surface of the BiVO₄ electrode for two reasons. First, we wanted to compare the performance of the photoelectrochemical Cl-recovery cell in neutral and acidic solutions and the TiO₂ protection layer increases the chemical stability of BiVO₄ in acidic solution. Second, we found that the surface of BiVO₄ forms BiOCl when BiVO₄ is immersed in a Cl-containing solution under illumination. The TiO2 coating layer prevents direct contact of Cl and BiVO₄ and can effectively suppress this undesired reaction. Detailed characterization of the conformal TiO2 coating layer on the surface of BiVO₄ can be found in a previous study where the deposition method of TiO2 was first reported [29]. Additionally, XPS results confirm the presence of the TiO₂ layer on the BiVO₄ surface (Fig. S9).

The previous study showed that the thin amorphous TiO_2 layer can effectively suppress the chemical dissolution of $BiVO_4$ in basic solutions while having a negligible effect on the photoelectrochemical properties [29]. We also note that the fact that the surfaces of $BiVO_4$ and TiO_2 are not catalytic for water oxidation is advantageous for utilizing photogenerated holes in the $BiVO_4/TiO_2$ photoanode for Cl^- oxidation [29].

Fig. 5a shows the V-t plot of the photoelectrochemical Cl-recovery cell composed of a BiOCl cathode and a BiVO₄/TiO₂ photoanode operated at 1 mA/cm² in 0.6 M NaCl under AM 1.5G, 100 mW/cm² illumination. The potential of the BiVO₄/TiO₂ electrode performing Cl⁻ oxidation (\sim 0.39 V vs Ag/AgCl) represents the Fermi level of the BiVO₄/TiO₂ electrode during the reaction under illumination. Since this potential is significantly more negative than the potential applied to the RuO_x anode in the electrochemical Cl-recovery cell, the voltage required to operate the cell was reduced from \sim -2.39 V to \sim -1.48 V. This clearly illustrates the advantage of utilizing solar energy harnessed by the BiVO₄ photoanode to operate the cell. When the same photoelectrochemical Cl-recovery cell was operated in 70 mM HCl, resulting in a decrease in the kinetic overpotential required by the BiOCl electrode, the cell voltage requirement was only \sim -0.72 V. Compared with the electrochemical cell operating in the same solution (Fig. 3b),

the use of the BiVO₄ photoanode resulted in a reduction of the cell voltage by 0.87 V. The V-t plots of the BiVO₄/TiO₂ electrode used for repeated cycles in the acidic solution are shown in Fig. S10 and confirm the stability of the BiVO₄/TiO₂ photoanode for use in the photoelectrochemical Cl-recovery cell. Additional photoelectrochemical properties of the BiVO₄/TiO₂ photoanode can be found in Fig. S11, showing the J-V plots of the BiVO₄/TiO₂ photoanode obtained in 0.6 M NaCl and 70 mM HCl using a three-electrode cell.

4. Conclusions

In summary, we have demonstrated the successful operation of various types of Cl-removal and Cl-recovery cells. In the Cl-removal cell, the Cl- storage reaction by Bi was coupled with either O2 reduction or H₂ evolution. When coupled with O₂ reduction, the Cl-removal cell generated electricity concurrently with Cl - removal. When coupled with H2 evolution, the Cl-removal cell generated H2 with a reduced thermodynamic energy requirement compared with that required by water splitting electrolysis cells. In the Cl-recovery cell, the Cl release reaction of BiOCl was coupled with Cl oxidation to generate Cl2 (acidic condition) or HOCl/ClO (neutral condition). We also demonstrated the operation of a proof-of-concept photoelectrochemical Clrecovery cell where the RuOx anode was replaced with a BiVO4/TiO2 photoanode that utilizes solar energy to reduce the energy required to operate the cell. The electrochemical and photoelectrochemical approaches reported in this study provide new energy-efficient strategies to selectively remove, recover, and valorize Cl while generating electricity or H2.

Declaration of Competing Interest

The authors declare that they have no known competing financial interests or personal relationships that could have appeared to influence the work reported in this paper.

Acknowledgements

This work was supported by the National Science Foundation (NSF) through grant CBET-1803496.

Appendix A. Supplementary data

Supplementary data to this article can be found online at https://doi.org/10.1016/j.cej.2020.126378.

References

- [1] V.R. Kelly, G.M. Lovett, K.C. Weathers, S.E.G. Findlay, D.L. Strayer, D.J. Burns, G.E. Likens, Long-term sodium chloride retention in a rural watershed: legacy effects of road salt on streamwater concentration, Environ. Sci. Technol. 42 (2008) 410–415
- [2] S.R. Corsi, L.A. De Cicco, M.A. Lutz, R.M. Hirsch, River chloride trends in snow-affected urban watersheds: increasing concentrations outpace urban growth rate and are common among all seasons, Sci. Total Environ. 508 (2015) 488–497.
- [3] J.P. Laceby, J.G. Kerr, D. Zhu, C. Chung, Q. Situ, S. Abbasi, J.F. Orwin, Chloride inputs to the North Saskatchewan River watershed: the role of road salts as a potential driver of salinization downstream of North America's northern most major city (Edmonton, Canada), Sci. Total Environ. 688 (2019) 1056–1068.
- [4] W.D. Hintz, R.A. Relyea, A review of the species, community, and ecosystem impacts of road salt salinisation in fresh waters, Freshwater Biol. 64 (2019) 1081–1097.
- [5] E.V. Novotny, A.R. Sander, O. Mohseni, H.G. Stefan, Chloride ion transport and mass balance in a metropolitan area using road salt, Water Resour. Res. 45 (2009) W12410.
- [6] G.E. Granato, L.A. DeSimone, J.R. Barbaro, L.C. Jeznach, Methods for evaluating potential sources of chloride in surface waters and groundwaters of the conterminous, United States: U.S. Geological Survey Open-File Report 2015-1080, (2015) 1-89. (Available at https://doi.org/10.3133/ofr20151080).
- [7] R. Scott, T. Goulden, M. Letman, J. Hayward, R. Jamieson, Long-term evaluation of

- the impact of urbanization on chloride levels in lakes in a temperate region, J. Environ. Manage. 244 (2019) 285–293.
- [8] A.M. Castillo, D.M.T. Sharpe, C.K. Ghalambor, L.F.D. Leon, Exploring the effects of salinization on trophic diversity in freshwater ecosystems: a quantitative review, Hydrobiologia 807 (2018) 1–17.
- [9] E.R. Herbert, P. Boon, A.J. Burgin, S.C. Neubauer, R.B. Franklin, M. Ardón, K.N. Hopfensperger, L.P.M. Lamers, P. Gell, A global perspective on wetland salinization: ecological consequences of a growing threat to freshwater wetlands, Ecosphere 6 (2015) 1–43.
- [10] S.S. Kaushal, P.M. Groffman, G.E. Likens, K.T. Belt, W.P. Stack, V.R. Kelly, L.E. Band, G.T. Fisher, Increased salinization of fresh water in the nrtheastern United States, Proc. Natl. Acad. Sci. 102 (2005) 13517–13520.
- [11] S.S. Kaushal, Increased salinization decreases safe drinking water, Environ. Sci. Technol. 50 (2016) 2765–2766.
- [12] U.S. Environmental Protection Agency, 1988. Ambient water quality criteria for chloride—1988. (Internet), (Washington, DC. Available at: https://www.epa.gov/ sites/production/files/2018-08/documents/chloride-aquatic-life-criteria-1988. ndf)
- [13] Chloride Compliance Study Nine Springs Wastewater Treatment Plant Final Report. 60329238; AECOM; Madison, WI, 2015 (Available at: https://www.madsewer.org/ Portals/0/ProgramInitiatives/ChlorideReduction/MMSD%20Chloride %20Compliance%20Study%20Report%20-%20Final%206-19-15bookmarks.pdf).
- [14] D.-Q. Ng, Y.-P. Lin, Chloride and sulfate concentrations on galvanic corrosion be tween lead and copper in drinking water, Environ. Chem. 13 (2016) 602–610.
- [15] D.A. Lytle, P. Sarin, V.L. Snoeyink, The effect of chloride and orthophosphate on the release of iron from a drinking water distribution system cast iron pipe, J. Water Supply Res Technol. –Aqua 54 (2005) 267–281.
- [16] E.G. Stets, C.J. Lee, D.A. Lytle, M.R. Schock, Increasing chloride in rivers of the conterminous U.S. and linkages topotential corrosivity and lead action level exceedances in drinking water, Sci. Total Environ. 613–614 (2018) 1498–1509.
- [17] M. Jaishankar, T. Tseten, N. Anbalagan, B.B. Mathew, K.N. Beeregowda, Mechanism and health effects of some heavy metals, Interdiscip. Toxicol. 7 (2014) 60–72
- [18] D.-H. Nam, K.-S. Choi, Bismuth as a new chloride-storage electrode enabling the construction of a practical high capacity desalination battery, J. Am. Chem. Soc. 139 (2017) 11055–11063.
- [19] D.-H. Nam, M.A. Lumley, K.-S. Choi, A desalination battery combining Cu₃[Fe (CN)₆]₂ as a Na-storage electrode and Bi as a Cl-storage electrode enabling membrane-free desalination, Chem. Mater. 31 (2019) 1460–1468.
- [20] C.R. Raj, A. Samanta, S.H. Noh, S. Mondal, T. Okajima, T. Ohsaka, T., Emerging new generation electrocatalysts for the oxygen reduction reaction, J. Mater. Chem. A 4 (2016) 11156–11178.
- [21] M. Kim, D.-H. Nam, H.-Y. Park, C. Kwon, K. Eom, S. Yoo, J. Jang, H.-J. Kim, E. Cho, Cobalt-carbon nanofibers as an efficient support-free catalyst for oxygen reduction reaction with a systematic study of active site formation, J. Mater. Chem. A 3 (2015) 14284–14290.
- [22] D.-H. Nam, K.-S. Choi, Electrochemical desalination using Bi/BiOCl electrodialysis cells, ACS Sustainable Chem. Eng. 6 (2018) 15455–15462.
- [23] D. Teschner, R. Farra, L. Yao, R. Schlögl, H. Soerijanto, R. Schomäcker, T. Schmidt, L. Szentmiklósi, A.P. Amrute, C. Mondelli, J. Pérez-Ramírez, G. Novell-Leruth, N. López, An integrated approach to deacon chemistry on RuO₂-based catalysts, J. Catal. 285 (2012) 273–284.
- [24] J. Pérez-Ramírez, C. Mondelli, T. Schmidt, O.F.-K. Schlüter, A. Wolf, L. Mleczko, T. Dreier, Sustainable chlorine recycling via catalysed HCl Oxidation: from fundamentals to implementation, Energy Environ. Sci. 4 (2011) 4786–4799.
- [25] R.K.B. Karlsson, A. Cornell, Selectivity between oxygen and chlorine evolution in the chlor-alkali and chlorate processes, Chem. Rev. 116 (2016) 2982–3028.
- [26] A.J. Bard, R. Parsons, J. Jordan, Standard potentials in aqueous solutions, Eds.; CRC Press (1985).
- [27] J.G. Vos, M.T.M. Koper, Measurement of competition between oxygen evolution and chlorine evolution using rotating ring-disk electrode voltammetry, J. Electroanal. Chem. 819 (2018) 260–268.
- [28] D.K. Lee, K.-S. Choi, Enhancing long-term photostability of BiVO₄ photoanodes for solar water splitting by tuning electrolyte composition, Nat. Energy 3 (2018) 53–60.
- [29] D. Lee, A. Kvit, K.-S. Choi, Enabling solar water oxidation by $BiVO_4$ photoanodes in basic media, Chem. Mater. 30 (2018) 4704–4712.
- [30] Y. Park, K.J. McDonald, K.-S. Choi, Progress in bismuth vanadate photoanodes for use in solar water oxidation, Chem. Soc. Rev. 42 (2013) 2321–2337.
- [31] D.K. Lee, D. Lee, M.A. Lumley, K.-S. Choi, Progress on ternary oxide-based photoanodes for use in photoelectrochemical cells for solar water splitting, Chem. Soc. Rev. 48 (2019) 2126–2157.
- [32] W. Luo, Z. Yang, Z. Li, J. Zhang, J. Liu, Z. Zhao, Z. Wang, S. Yan, T. Yu, Z. Zou, Solar hydrogen generation from seawater with a modified BiVO₄ photoanode, Energy Environ. Sci. 4 (2011) 4046–4051.
- [33] S. Iguchi, Y. Miseki, K. Sayama, Efficient Hypochlorous Acid (HClO) Production via photoelectrochemical solar energy conversion using a BiVO₄-based photoanode, Sustain. Energy Fuels 2 (2018) 155–162.
- [34] A.M. Rassoolkhani, W. Cheng, J. Lee, A. McKee, J. Koonce, J. Coffel, A. Ghanim, H.G.A. Aurand, C.S. Kim, W.I. Park, H. Jung, S. Mubeen, Nanostructured bismuth vanadate/tungsten oxide photoanode for chlorine production with hydrogen generation at the dark cathode, Commun. Chem. 2 (2019) 57.
- [35] M. Oghbaei, O. Mirzaee, Microwave versus conventional sintering: a review of fundamentals, advantages and applications, J. Alloys Compd. 494 (2010) 175–189.